Understanding the Conformational Stability and Electronic Structures of Modified Polymers Based on Polythiophene

Sung Y. Hong and Dennis S. Marynick*

Department of Chemistry, The University of Texas at Arlington, Arlington, Texas 76019-0065

Received February 20, 1992; Revised Manuscript Received May 5, 1992

ABSTRACT: Conformations and electronic structures of polymers based on polythiophene with various fused fragments were theoretically investigated. Thioethylenic, thiodimethylenic, and ethylenic fragments were explored, yielding polythieno[3,4-*b*]thiophene, polythieno[3,4-*c*]thiophene, and poly(3-thiabicyclo[3.2.0]-1,4,6-heptatriene), respectively. A conformational study, using the method of partial retention of diatomic differential overlap, was performed to ascertain the relative stability of the aromatic vs quinoid forms as well as the torsional potentials of the aromatic forms. The electronic structures of the polymers were obtained through modified extended-Hückel band calculations. It was found that the stability of a conformer is mainly governed by the electronic effects associated with a given fragment. The more stable conformer of a polymer has a lower highest occupied crystal orbital level, a larger band gap, and a smaller highest valence bandwidth. The symmetries and the relative energy levels of the frontier orbitals of a fragment compared to those of a parent polymer play important roles in determining the electronic effects of a fragment and, in turn, the stability of a conformer. It is expected that polythieno[3,4-*b*]thiophene should be a very promising conducting polymer whose band gap is predicted to be comparable to that of polyacetylene.

Introduction

Heterocyclic polymers such as polythiophene (PT), polypyrrole (PPy), polyfuran (PF), and their derivatives have attracted much attention recently because of their electrical properties and relatively good environmental stabilities. Because of the good physicochemical properties of these heterocyclic polymers, many experimental[1-9] and theoretical efforts[10-16] have been focused on the modification of their chemical structures toward very small band gap polymers, which would be intrinsically good electrical conductors. In particular, modified polymers based on PT have been major targets for achieving such a goal because of the intrinsically small band gap of PT and the ease of the electrochemical preparations of films. We have previously shown that the intrinsic electronic effect of the heteroatom is to raise the band gap relative to polyacetylene and that the relatively small band gap of PT arises from the fact that sulfur exhibits a smaller electronic effect in PT than does nitrogen in polypyrrole or oxygen in polyfuran.[17]

Polymers based on *cis*-polyacetylene (PA) backbones such as poly(*p*-phenylene) (PPP), the heterocyclic polymers mentioned above, and their derivatives are *nondegenerate* in their ground states and possess two types of possible conformations: aromatic and quinoid.

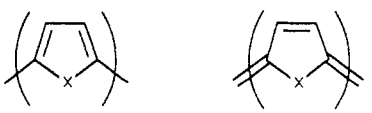

Aromatic Quinoid

Earlier theoretical work has shown that poly(*p*-phenylene), polythiophene, and polypyrrole are aromatic in their ground states and are subject to structural modifications toward quinoid forms upon charge transfer.[18] Also, a quinoid form of polythiophene with $\delta r = 0.06$ Å is predicted to possess a near-zero band gap.[11] Here δr is defined as the average value of the bond length alternation along the backbone of the polymer. Therefore, a potential way to design a small band gap polymer is to modify the chemical structure of a polymer toward a quinoid form. In this context, experimental and theoretical attempts have been made to incorporate the quinoid forms by inserting methene (–CR=) groups into a polymeric backbone[2,10,16] or by attaching rings onto the parent rings.[1,6,9,11-15] On the basis of theoretical calculations, Bredas[11] has proposed that polyisonaphthothiophene (PINT), polyisothianaphthene (PITN), and polythieno[3,4-*c*]thiophene (PTcT) are good candidates for electrically conducting polymers. Bredas calculated the structures of these systems via monomer or dimer optimizations, with the oligomer terminated with one hydrogen at each terminal position. This procedure clearly biases the calculated geometry toward the aromatic form.[19] The VEH method was then employed to calculate the band gaps of PITN, PINT, and PTcT, which were found to be 0.54, 0.01, and 1.02 eV, respectively. Bredas attributed the decrease in band gap relative to polythiophene to an increase in the quinoid contribution to the electronic structure. However, more recent work[12,15,19] has pointed out the importance of conformational effects in determining band gaps of such polymers. Lee et al. employed MNDO band calculations and claimed that these polymers are quinoidal in their ground states, with the predicted band gaps of 1.16, 1.50, and 2.00 eV at the Hückel level.[12,15] Other theoretical[19] and experimental[20] work also supports the quinoid form of PITN in the ground state. Therefore, whenever we deal with polymers based on *cis*-PA backbones which are nondegenerate in their ground states, the relative stability of conformers of such polymers becomes a critical issue.

Is there any simple way to predict the relative stability of aromatic vs quinoid forms before performing complicated calculations? In this study we try to answer this question by elucidating how fragments fused onto PT affect the relative stability of the conformers and their electronic structures. Selected polymers include polythieno[3,4-*b*]thiophene (PTbT), PTcT, and poly(3-thiabicyclo[3.2.0]-1,4,6-heptatriene) (PTBH) (Figure 1). To our knowledge, none of these polymers have been synthesized yet. We examine the relative stabilities of the conformers (aromatic and quinoid forms) as well as the torsional potential curves of the aromatic forms using the method of partial retention of diatomic differential overlap (PRDDO).[21] The electronic structures of the conformers

0024-9297/92/2225-4652$03.00/0

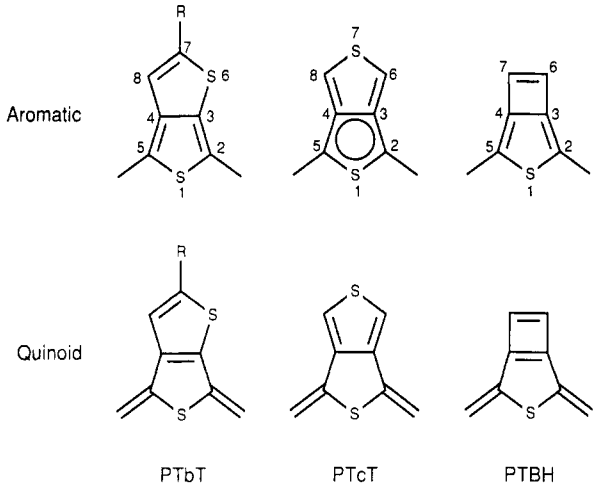

Figure 1. Aromatic and quinoid forms of polythieno[3,4-*b*]thiophene (PTbT), polythieno[3,4-*c*]thiophene (PTcT), and poly(3-thiabicyclo[3.2.0]-1,4,6-heptatriene) (PTBH). Numbering is the same for the quinoid forms.

are computed using the modified extended-Hückel (EH) method.[17]

Torsional Potential Curves of the Aromatic Forms

The length of π-electron delocalization along the polymeric backbone plays a crucial role in determining the electrical properties of conjugated polymers. Experimental observations of a decrease in optical gaps with increasing size of thiophene oligomers[22,23] reflect the effect of the length of π-electron delocalization on the electronic properties of conjugated polymers. In addition to polymeric chain lengths, the degree of coplanarity of conjugated aromatic polymers is another factor which affects π-electron delocalization. A theoretical investigation[24] of PPP, PT, and PPy demonstrated that as two adjacent rings deviate from coplanarity, ionization potentials and band gap values increase and the widths of the highest occupied bands decrease in accord with a cosine law.

Because of the relatively large size of the van der Waals radius of sulfur, PT-related polymers may have significantly different torsional potentials about the inter-ring bond when compared to their oxygen-containing analogues.[19,25-27] In this connection, we examined the torsional behavior of the aromatic forms of the polymers in Figure 1 by constructing the potential energy surfaces of the corresponding dimers:

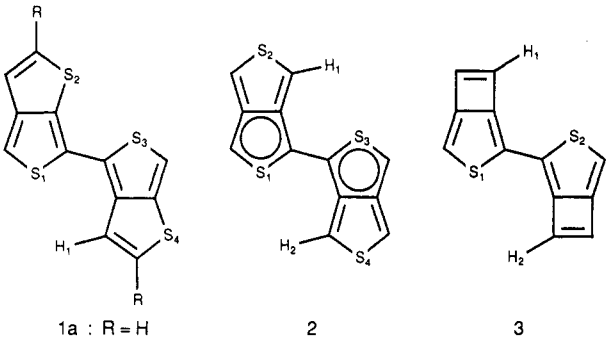

The total energy calculations were carried out with torsional angles (θ) of 0° (syn) to 180° (anti) in increments of 30° using the PRDDO method. The inter-ring parameters (bond lengths and angles) were optimized at each θ value. Since detailed intra-ring structures do not significantly affect relative energetics of rotational conformers,[28]

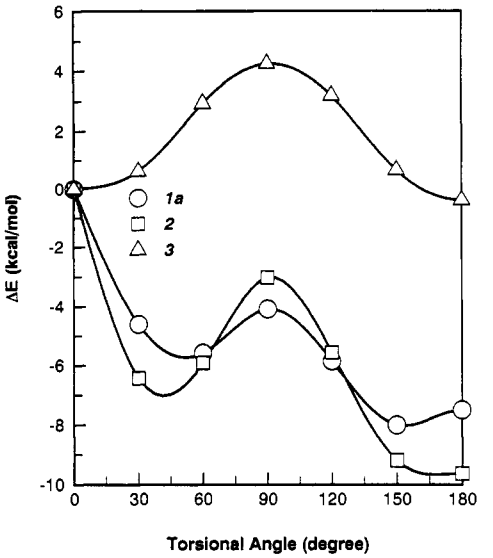

Figure 2. Torsional potential curves of the dimers **1a** (bithieno[3,4-*b*]thiophene), **2** (bithieno[3,4-*c*]thiophene), and **3** (bi(3-thiabicyclo[3.2.0]-1,4,6-heptatriene)).

the intra-ring parameters for the monomers optimized by PRDDO were used throughout the calculations for computational efficiency. The PRDDO method has been shown to be a useful tool for predicting conformations as well as geometries of relatively large molecules,[19,27,28] while semiempirical methods of the neglect of diatomic overlap type (such as MNDO and CNDO) are often unrealistic in favoring perpendicular conformations for systems with partial conjugation.[28,29]

In Figure 2, torsional energy surfaces for the dimers **1a**, **2**, and **3** are shown. The torsional behaviors of **1a** and **2** are similar. The syn conformers are the most unstable because of steric repulsions between neighboring rings. The distances between the S1 and S3 atoms and between the S2 and H1 atoms of **1a** are 2.95 and 2.39 Å, respectively. These values are much smaller than the sum of the van der Waals radii of the corresponding atoms (1.85 Å for S and 1.2 Å for H).[30] The S1–S3 and H1–H2 distances in **2** are 2.91 and 1.67 Å, respectively. A local minimum is found around 45° and a local maximum at 90°. This is the result of competition between the effects of conjugation, which favor a coplanar structure, and steric repulsions. Even though the 150°-twisted structure of **1a** appears more stable than the anti-coplanar structure, full optimizations for both structures revealed that the latter structure is essentially degenerate with the former (ΔE = 0.2 kcal/mol). The flatness of the potential curves for the dimers **1a** and **2** in the range of 150–180° arises from a compromise between the effects of conjugation and the steric repulsions between S2 and S3 and between S1 and H1 in **1a** or between S1 and H2 (S3 and H1) in **2**. The S2–S3 and S1–H1 distances of the anti form of **1a** are 3.23 and 2.74 Å, respectively. The S1–H2 (S3–H1) distance of the anti form of **2** is 2.63 Å. **1b** with R = CH_3 shows almost the same torsional surface as **1a**. The potential curve for **3** is quite different from the others, showing almost the same preferences for the syn and anti conformations and a maximum at θ = 90°. The anti form is predicted to be slightly (~0.4 kcal/mol) more stable than the syn form, while the torsional barrier is estimated to be 4.6 kcal/mol. This suggests a considerable population of the syn form in the polymer PTBH. A similar situation was observed from the NMR study of bithiophene in a nematic phase of a crystalline solvent.[31] The S1–S2 and H1–H2 distances of the syn form are 3.31 and 2.89 Å, respectively, while the

Table I
Relative Stabilities (kcal/mol) of the Aromatic vs Quinoid Forms for PT, PTbT, PTcT, and PTBH as a Function of the Chain Length[a]

chain length	thiophene[b]	ITN[c]	TbT	7m-TbT	TcT	TBH
1	37.4	11.9	21.8	22.2	-28.1	55.6
2	24.2	3.8	11.1	11.3	-33.6	44.7
3	19.8	1.6	7.5	7.9	-34.1	40.7
4	17.4	0.5	5.7	6.5	-33.1	39.1
5	16.1	-0.1				
6	15.2	-1.6				
∞	10.6	-2.4	0.3	2.0	-30.5	33.5

[a] All geometrical optimizations were performed at the PRDDO level. [b] Data for the thiophene and isothianaphthene oligomers were obtained from ref 19. [c] The aromatic forms are nonplanar with a torsional angle of 58.7°.

S1-H2 (S2-H1) distance of the anti form is 3.65 Å.

Relative Stability of the Aromatic vs Quinoid Forms

Since it was demonstrated that a band gap of a *nondegenerate* conjugated polymer in the ground state is related to the energetics of the conformations,[15,19] the relative stability of the aromatic vs quinoid forms becomes a critical issue for designing new conducting polymers. We have successfully tackled this issue for a number of PT-related polymers through oligomer calculations.[19] The scheme to obtain the relative stability of aromatic vs quinoid forms from oligomer calculations is briefly given here. For the details, the reader is referred to ref 19. First, optimized structures of the oligomers of interest, extending from monomers up to tetramers or higher, are calculated for both forms. Quinoid forms can be modeled by attaching two hydrogens at each of the terminal atoms, while aromatic forms have one hydrogen. Second, we approximate the energy difference between the two forms *in the absence of end groups* as a function of chain length, N, according to eq 1, where E_q and E_a are the total energies

$$\Delta E_{qa}^N = E_q^N - E_a^N - 2E_H + 2E_{CH} \quad (1)$$

of the quinoid and aromatic forms, respectively. E_H is the hydrogen atomic energy, -0.4712 au, and E_{CH} is the average C-H bond dissociation energy, 90.3 kcal/mol. Finally, we extrapolate the energy difference per chain length, $\Delta E_{qa}^N/N$, using eq 2. The relative stability of the two forms of a polymer amounts to the value of a_0.

$$\Delta E_{qa}^N/N = a_0 + a_1/N + a_2/N^2 \quad (2)$$

We used the same scheme for the polymers of interest in this study. Geometrical structures of the oligomers up to the trimers were obtained by performing full PRDDO optimizations, except for the C-H bond lengths. The C(sp^3)-H and C(sp^2)-H bond lengths were fixed at 1.10 and 1.08 Å, respectively. All aromatic conformers were considered to be anti-coplanar. The total energy calculations for the tetramers were performed with the structures extracted from the trimer optimizations. In Table I, calculated $\Delta E_{qa}^N/N$ values for the oligomers including thiophene and isothianaphthene are shown, along with the values extrapolated to the infinite chain limit ($N = \infty$). It is quite obvious that the ground-state geometries of PT and PTBH are aromatic, while that of PTcT is quinoidal. This prediction is consistent with MNDO band calculations.[15] For PITN, a theoretical calculation[15] by Lee et al. favors the quinoid form, which is opposite to the prediction[11] of Bredas. PRDDO calculations predicted that the quinoid form is slightly more stable than even the nonplanar aromatic form.[19] A recent ^{13}C cross-polarization/magic angle spinning nuclear magnetic resonance investigation supports a quinoid form for PITN.[20] The quinoid form of PTbT is predicted to have a stability comparable with that of the aromatic form. The introduction of an alkyl group to PTbT is accompanied by a weak tendency to increase the stability of the aromatic form over the quinoid form.

Table II
Geometrical Parameters (Bond Lengths in Angstroms and Bond Angles in Degrees) Used for Extended-Hückel Band Calculations[a]

geom param	PTbT (A)	PTbT (Q)	PTcT (A)	PTcT (Q)	PTBH (A)[b]	PTBH (Q)
1-2	1.731	1.779	1.717	1.767	1.784 (1.794)	1.786
2-3	1.348	1.463	1.433	1.461	1.321 (1.367)	1.428
3-4	1.429	1.350	1.443	1.438	1.436 (1.440)	1.306
4-5	1.352	1.482	1.433	1.461	1.321 (1.367)	1.428
3-6	1.735	1.711	1.347	1.330	1.502 (1.515)	1.542
6-7	1.738	1.714	1.688	1.708	1.331 (1.375)	1.316
7-8	1.315	1.688	1.688	1.706		
2-2′	1.453	1.327	1.393	1.331	1.454	1.329
1-5-4	109.5	106.8	107.8	107.5	107.8 (103.5)	104.9
2-3-4	114.1	116.8	113.5	114.2	115.8 (115.5)	117.7
3-4-5	113.5	114.7	113.5	114.2	115.8 (115.5)	117.7
4-3-6	110.8	112.0	111.6	111.9	88.0 (89.3)	90.2
3-6-7	90.8	90.8	112.2	112.7	92.0 (91.1)	89.8
6-7-8	114.7	112.7	92.4	90.8		
3-2-2′	129.6	129.0	128.4	129.2	130.5	129.7

[a] See Figure 1 for the definition for the geometrical parameters. [b] X-ray crystallographic structural parameters of 6,7-diphenyl-3-thiabicyclo[3.2.0]heptatriene from ref 33.

Electronic Structures

Geometrical parameters for the polymers in Figure 1 were selected from those for the middle rings of the corresponding trimers and are given in Table II. For comparison, the experimental parameters are included for the monomer of 6,7-diphenyl-3-thiabicyclo[3.2.0]-heptatriene. The electronic structures were obtained by performing modified EH band calculations[17] on the planar polymers (it is not expected that deviations from planarity of the order of a few degrees would significantly affect the calculated band gaps). The modified EH method employs off-diagonal elements of the form

$$H_{ij}^{\alpha\beta} = K_1(H_{ii}^{\alpha\alpha} + H_{jj}^{\beta\beta}) \exp(-K_2 R^{\alpha\beta}) S_{ij}^{\alpha\beta} \quad (3)$$

where K_1 and K_2 are adjustable parameters, determined to be 1.41 and 0.13Å^{-1}, respectively. $H_{ii}^{\alpha\alpha}$ is the energy integral which is assumed to be equal to the energy of an electron in the ith atomic orbital (AO) of the isolated atom α in the appropriate state. $S_{ij}^{\alpha\beta}$ is the overlap between the ith AO of a center α and the jth AO of a center β, and $R^{\alpha\beta}$ is the distance between two centers α and β. The method is parametrized to reproduce band gaps defined as the π-π^* λ_{max} of the optical spectra of conjugated polymers. It includes separate parameters for PRDDO and MNDO optimized geometries and has been shown to yield remarkably reliable band structures for a wide variety of conjugated polymers, including those with heteroatoms. We used the sulfur atomic parameters as previously defined for PRDDO geometries: 2.217 for the valence orbital exponents and 13.3 eV for the valence-state ionization potentials of the 3p orbitals.[17]

The predicted electronic properties of the polymers including PT, PITN, and PINT are summarized in Table III. More stable forms of the polymers tend to have lower

Table III
Comparison of the Predicted Electronic Properties of PT, PTbT, PTcT, PTBH, PITN, and PINT

polymer[a]		E_g (eV)[b]	E_f (eV)	highest valence band width (eV)	δr[c]
PT	(A)[d]	2.61 (2.5–2.7)	−11.06	2.23	0.10
	(Q)	1.39	−10.40	3.14	−0.16
PTbT	(A)	1.54	−10.13	2.72	0.09
	(Q)	1.63	−10.19	2.79	−0.13
7m-TbT	(A)	1.50	−10.05	2.69	0.09
	(Q)	1.48	−10.05	2.79	−0.12
PTcT	(A)	2.54	−10.21	1.96	−0.03
	(Q)	3.69	−10.75	1.61	−0.08
PTBH	(A)	4.34	−11.90	0.05	0.12
	(Q)	0.83	−10.13	2.11	−0.11
PITN	(A)[e]	0.80	−10.10	3.18	0.10
	(Q)	2.28 (1.4, 2.0)	−10.72	2.79	−0.13
PINT	(A)[f]	0.37	−9.91	2.56	0.12
	(Q)	2.77 (2.1)	−10.81	1.58	−0.13

[a] All geometrical parameters were obtained from the PRDDO optimizations. [b] Values in parentheses are obtained from the optical peaks for π–π^* transitions: ref (34 for PT, ref 35 for PITN, and ref 6 for PINT. [c] An average value of the bond alternation, defined as $\delta r = [R(2\text{–}5') - R(3\text{–}2) + R(4\text{–}3) - R(5\text{–}4)]/2$ (see Figure 1 for numberings). [d] Underlined is the most stable conformer, except for PTbT, whose aromatic and quinoid forms are essentially equal in energy. [e] E_g for the nonplanar (58.7° twisted) form is calculated to b 2.25 eV. [f] E_g for the nonplanar (58.7° twisted) form is calculated to be 1.55 eV.

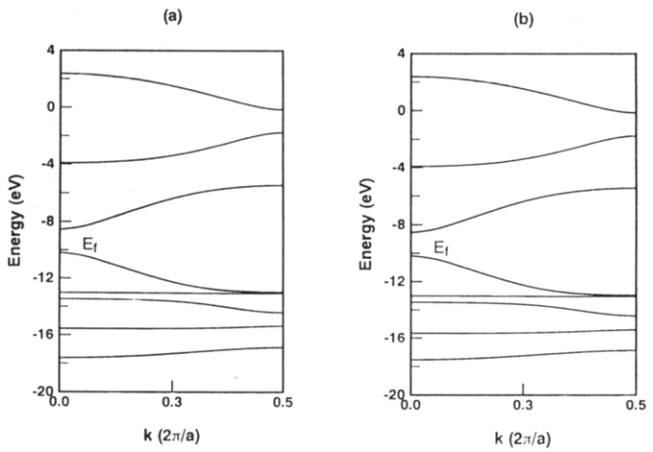

Figure 3. π-Band structures of the (a) aromatic and (b) quinoid forms of polythieno[3,4-*b*]thiophene.

Fermi levels (lower levels of the highest occupied crystal orbital), larger band gaps, and smaller bandwidths. Because the values of the bond alternation δr of these polymers do not deviate much from those of PT, except for the case of PTcT, it is expected that the variation of the band gaps mainly arises from the electronic perturbations produced by the fusion of fragments onto the rings. Evolutions of the band gaps by attaching fragments onto PT have been demonstrated for PITN and for PTBH.[12,15,32]

The similar electronic properties of the aromatic and quinoid forms of PTbT reflect the negligible difference in energy between these forms. The predicted π-band structures for both forms of PTbT are very similar (Figure 3). However, the interactions of the PT backbone with the fragment are different near the Fermi level (Figure 4). In the aromatic form, the HOCO of PTbT is destabilized by ca. 1.0 eV by the interaction between the HOCO of PT and the highest occupied molecular orbital (HOMO) (π_2) of the thioethylenic fragment, while the lowest unoccupied crystal orbital (LUCO) is barely stabilized (ca. 0.1 eV) because the stabilization due to the bonding interaction of the LUCO of PT with the π_3 fragment orbital is almost

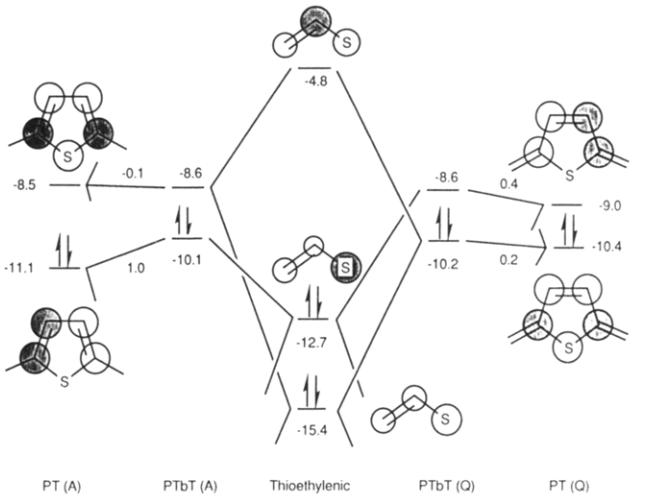

Figure 4. Orbital correlation diagram near the Fermi level of polythieno[3,4-*b*]thiophene for the interactions of the polythiophene backbone with the thioethylenic fragment.

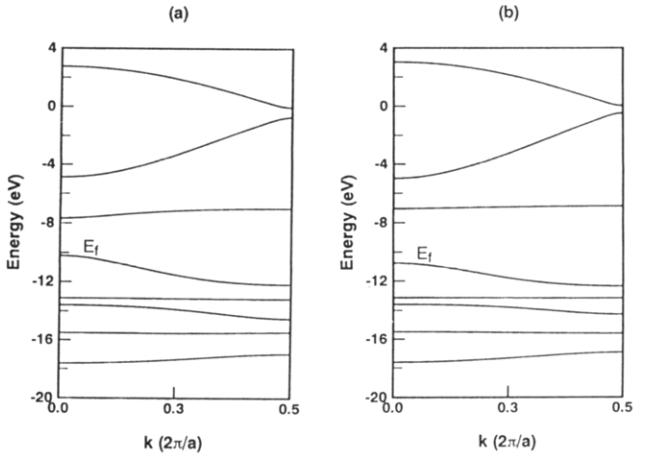

Figure 5. π-Band structures of the (a) aromatic and (b) quinoid forms of polythieno[3,4-*c*]thiophene.

cancelled out by the mixing of the π_1 fragment orbital. Since the symmetries of the HOCO and LUCO of PT are interchanged upon going from the aromatic to the quinoid form, the HOCO of quinoid PTbT arises from the interaction of the HOCO of PT with the π_1 and π_3 fragment orbitals. This orbital is slightly destabilized (ca. 0.2 eV) because the π_1 orbital is slightly closer in energy to the HOCO than is the π_3 orbital. The LUCO is also destabilized (ca. 0.4 eV) by the interaction of the LUCO of quinoid PT with the HOMO (π_2) of the fragment. It should be stressed that the strong interaction of the π_1 orbital of a fragment with the crystal orbitals near the Fermi level plays an important role in determining the relative stabilities and the electronic structures of these systems.

The predicted π-band structures for both forms of PTcT are shown in Figure 5. Mixings of the orbitals of the same symmetry with respect to the mirror plane perpendicular to the translational axis are found at the center and edge of the Brillouin zone. The interactions of the PT backbone with the thiodimethylenic fragment are essentially the same as in the case of PTbT. However, the π_2 and π_3 levels of the thiodimethylenic fragment are so close in energy to those of the HOCO and LUCO of PT, respectively, that the interactions near the Fermi level are very strong, depressing the effect of the π_1 orbital and resulting in band crossing and a relatively large band gap in the case of the aromatic form. As in Figure 6, the HOCO of aromatic PTcT mainly arises from the stabilization of the

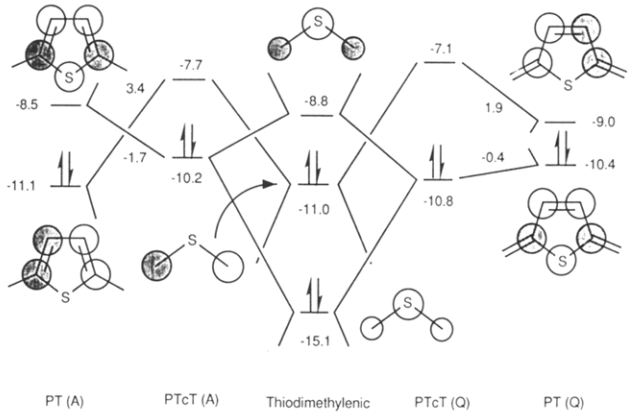

Figure 6. Orbital correlation diagram near the Fermi level of polythieno[3,4-*c*]thiophene for the interactions of the polythiophene backbone with the thiodimethylenic fragment.

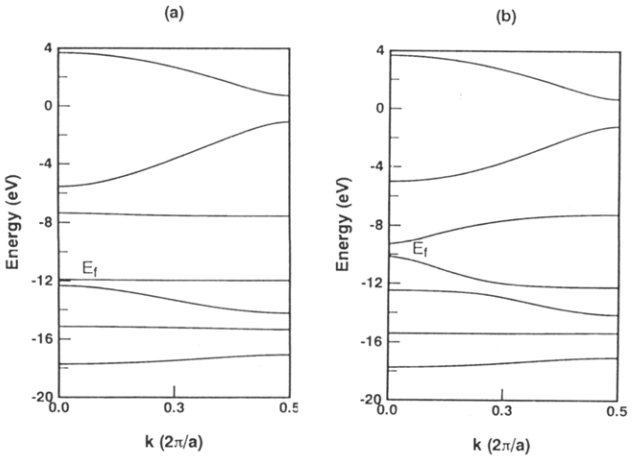

Figure 7. π-Band structures of the (a) aromatic and (b) quinoid forms of poly(3-thiabicyclo[3.2.0]-1,4,6-heptatriene).

LUCO of PT through the interaction with the π_3 orbital of the fragment. The LUCO of PT strongly interacts with the HOMO (π_2) of the fragment so that the resultant LUCO of PTcT is highly elevated. The strong coupling of the thiodimethylenic fragment with the parent backbone induces a geometrical relaxation toward quinoid-like bond alternations, as seen in Table III. This results in the further stabilization of the HOCO and destabilization of the LUCO. In the case of quinoid PTcT, the HOCO is stabilized because the π_3 level is closer to the HOCO of PT than is the π_1 level and the LUCO is strongly destabilized by the antibonding interaction of the LUCO of PT with the HOMO (π_2) of the fragment. The lowest conduction bands of both forms are flat along the k-momentum axis. The LUCOs of both conformers at the edge of the Brillouin zone ($k = \pi/a$) arise from an antibonding interaction between the HOCO of PT at $k = \pi/a$ and the π_3 orbital of the fragment.

Our predicted π-band structures for both PTBH conformers (Figure 7) show the band gaps at the center of the Brillouin zone while those of Hückel calculations by Lee et al. show them at the edge.[15] Therefore, the interactions near the Fermi level in Figure 8 are different from those calculated by Lee et al. Because the symmetry of the HOMO and the LUMO of the ethylenic fragment is different from the corresponding MO of the other fragments, the interactions of the PT backbone with the ethylenic fragment near the Fermi level is also different from those in the case of PTbT or PTcT, showing opposite trends of band gaps induced by the fragment. The HOCO of the aromatic form is stabilized by interacting in a

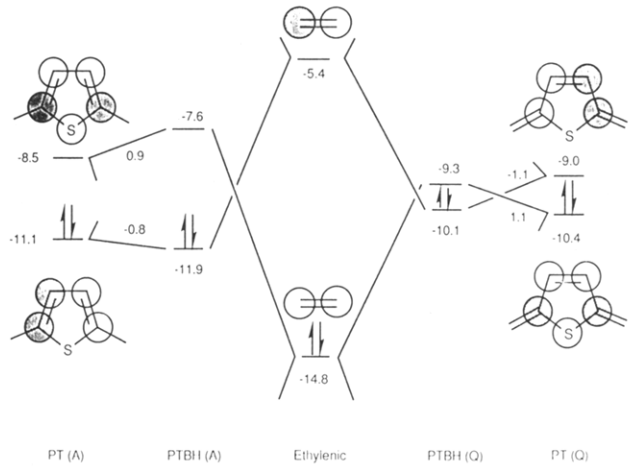

Figure 8. Orbital correlation diagram near the Fermi level of poly(3-thiabicyclo[3.2.0]-1,4,6-heptatriene) for the interactions of the polythiophene backbone with the ethylenic fragment.

bonding way with the LUMO of the ethylenic fragment while the LUCO is pushed up by interacting in an antibonding way with the HOMO of the fragment, resulting in a larger band gap. In the case of the quinoid form, the HOCO results from the bonding interaction of the LUCO of quinoid PT with the LUMO of the fragment and the LUCO arises from the antibonding interaction of the HOCO of quinoid PT with the HOMO of the fragment. The lowest conduction band and highest valence band of the aromatic form are very flat. The crystal orbitals at $k = \pi/a$ near the Fermi level are the same as those[15] of Lee et al. This is not true in the case of the quinoid form probably because of the different bond lengths between the fragment and the PT backbone: the PRDDO optimized geometry shows the longer bond length (1.542 Å) than the MNDO geometry (1.360 Å) as shown in the following:

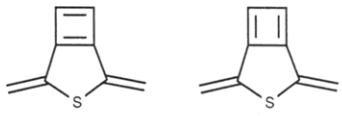

Conclusion

It is found that the relative stability of aromatic vs quinoid forms of these polymers is mainly governed by the electronic effects of a fragment fused onto the PT ring and that conformers with larger band gaps are usually more stable. The magnitude of the electronic effect depends on the symmetries and the relative energy levels of the frontier orbitals of a fragment compared to those of PT. Symmetry-based arguments show that when the HOCO (LUCO) of the parent polymeric backbone of a conformer interacts with the LUMO (HOMO) of a fragment, the conformer is generally stabilized, as found for quinoid PTcT and aromatic PTBH. However, when there are strong interactions of crystal orbitals near the Fermi level with frontier orbitals other than the HOMO and LUMO of a fragment, the effect of symmetry on the stability can be strongly depressed and the prediction may be difficult, as in the case of PTbT.

Aromatic forms of the polymers investigated in this study are predicted to be coplanar. Among those polymers, PTbT is expected to be a very promising conductive polymer whose predicted band (π–π^* λ_{max}) gap (1.5–1.6 eV) is comparable to that of *trans*-PA. Both conformers of PTbT have comparable stabilities and similar electronic properties.

Acknowledgment. This work was supported by the Defense Advanced Research Projects Agency, monitored by the Office of Naval Research, and the Robert A. Welch Foundation (Grant Y-743).

References and Notes

(1) Wudl, F.; Kobayashi, M.; Heeger, A. J. *J. Org. Chem.* **1984**, *49*, 3382.
(2) Jenekhe, S. A. *Nature* **1986**, *322*, 345.
(3) An, H.; Seki, M.; Yosomiya, R. *Makromol. Chem., Rapid Commun.* **1987**, *8*, 325.
(4) Bolognesi, A.; Catellani, M.; Destri, S.; Zamboni, R.; Taliani, C. *J. Chem. Soc., Chem. Commun.* **1988**, 246.
(5) Hagiwara, T.; Yamaura, M.; Sato, K.; Hirasaka, M.; Iwata, K. *Synth. Met.* **1989**, *32*, 367.
(6) Ikenoue, Y. *Synth. Met.* **1990**, *35*, 263.
(7) Ueda, M.; Miyaji, Y.; Ito, T.; Oba, Y.; Sona, T. *Macromolecules* **1991**, *24*, 2694.
(8) Ohshita, J.; Kanaya, D.; Ishikawa, M.; Koieke, T.; Yamanaka, T. *Macromolecules* **1991**, *24*, 2106.
(9) Ikenoue, Y.; Wudl, F.; Heeger, A. J. *Synth. Met.* **1991**, *40*, 1.
(10) Kertesz, M.; Lee, Y.-S. *J. Phys. Chem.* **1987**, *91*, 2690.
(11) Bredas, J. L. *Synth. Met.* **1987**, *17*, 115.
(12) Lee, Y.-S.; Kertesz, M. *J. Chem. Phys.* **1988**, *88*, 2609.
(13) Kertesz, M.; Lee, Y.-S. *Synth. Met.* **1989**, *28*, C545.
(14) Otto, P.; Ladik, J. *Synth. Met.* **1990**, *36*, 327.
(15) Lee, Y.-S.; Kertesz, M.; Elsenbaumer, R. L. *Chem. Mater.* **1990**, *2*, 526.
(16) Toussaint, J. M.; Bredas, J. L. *J. Chem. Phys.* **1991**, *94*, 8122.
(17) Hong, S. Y.; Marynick, D. S. *J. Chem. Phys.* **1992**, *96*, 5497.
(18) Bredas, J. L.; Themans, B.; Fripiat, J. G.; Andre, J. M.; Chance, R. R. *Phys. Rev. B* **1984**, *29*, 6761.
(19) Nayak, K.; Marynick, D. S. *Macromolecules* **1990**, *23*, 2237.
(20) Hoogmartens, I.; Vanderzande, D.; Martens, H.; Gelan, J. *Synth. Met.* **1991**, *41–43*, 513.
(21) Halgren, T. A.; Lipscomb, W. N. *J. Chem. Phys.* **1973**, *58*, 1569. Marynick, D. S.; Lipscomb, W. N. *Proc. Natl. Sci. U.S.A.* **1982**, *79*, 1341.
(22) Navarrete, J. T. L.; Tian, B.; Zerbi, G. *Synth. Met.* **1990**, *38*, 299.
(23) Fichou, D.; Horowitz, G.; Xu, B.; Garnier, F. *Synth. Met.* **1990**, *39*, 243.
(24) Bredas, J. L.; Street, G. B.; Themans, B.; Andre, J. M. *J. Chem. Phys.* **1985**, *83*, 1323.
(25) Almenningen, A.; Bastiansen, O.; Svendsas, P. *Acta Chem. Scand.* **1955**, *12*, 1671.
(26) van Bolhuis, F.; Wynberg, H.; Havinga, E. E.; Meijer, E. W.; Staring, E. G. J. *Synth. Met.* **1989**, *30*, 381.
(27) Reynolds, J. R.; Ruiz, J. P.; Child, A. D.; Nayak, K.; Marynick, D. S. *Macromolecules* **1991**, *24*, 678.
(28) Hong, S. Y.; Marynick, D. S., submitted to *Macromolecules*.
(29) Barone, V.; Lelj, F.; Cauletti, C.; Piancastelli, M. N.; Russo, N. *Mol. Phys.* **1983**, *49*, 599. Perahia, D.; Pullman, A. *Chem. Phys. Lett.* **1973**, *19*, 73.
(30) *CRC Handbook of Chemistry and Physics*, 70th ed.; Weast, R. C., Lide, D. R., Astle, M. J., Beyer, W. H., Eds.; CRC Press Inc.: Boca Raton, FL 1990.
(31) Bucci, P.; Longeri, M.; Veracini, C.; Lunazzi, L. *J. Am. Chem. Soc.* **1974**, *96*, 1305.
(32) Bredas, J. L.; Heeger, A. J.; Wudl, F. *J. Chem. Phys.* **1986**, *85*, 4673.
(33) Garratt, P. J. *Pure Appl. Chem.* **1975**, *44*, 783.
(34) Kaneto, K.; Yoshino, K.; Inuishi, Y. *Solid State Commun.* **1983**, *46*, 389. Chung, T.-C.; Kasufman, J. H.; Heeger, A. J.; Wudl, F. *Phys. Rev. B.* **1984**, *30*, 702.
(35) Chandrasekhar, P.; Masulaitis, A. M.; Gumbs, R. W. *Synth. Met.* **1990**, *36*, 303. Kobayashi, M.; Colaneri, N.; Boysel, M.; Wudl, F.; Heeger, A. J. *J. Chem. Phys.* **1985**, *82*, 5717.

Registry No. **1a**, 142189-42-2; **1a** (dimer), 142189-48-8; **1a** (trimer), 142189-49-9; **1a** (tetramer), 142189-50-2; **1a** (homopolymer), 142189-51-3; **1b**, 142189-43-3; **1b** (dimer), 142189-52-4; **1b** (trimer), 142189-53-5; **1b** (tetramer), 142189-54-6; **1b** (homopolymer), 142189-55-7; **2**, 142189-44-4; **2** (dimer), 142189-56-8; **2** (trimer), 142189-57-9; **2** (tetramer), 142189-58-0; **2** (homopolymer), 142189-59-1; **3**, 142189-45-5; **3** (dimer), 142189-60-4; **3** (trimer), 142189-61-5; **3** (tetramer), 142189-62-6; **3** (homopolymer), 142189-63-7; ITN (homopolymer), 91201-85-3; PINT (homopolymer), 107949-39-3; thiophene (homopolymer), 25233-34-5.